S-system theory applied to array-based GNSS ionospheric sensing

AMIR KHODABANDEH[1] AND PETER J.G. TEUNISSEN[1,2]

1 GNSS Research Centre, Department of Spatial Sciences, Curtin University of Technology, Perth, Australia (amir.khodabandeh@curtin.edu.au)

2 Department of Geoscience and Remote Sensing, Delft University of Technology, Delft, The Netherlands (p.teunissen@curtin.edu.au)

Received: July 27, 2016; Revised: October 10, 2016; Accepted: October 31, 2016

ABSTRACT

The GPS carrier-phase and code data have proven to be valuable sources of measuring the Earth's ionospheric total electron content (TEC). With the development of new GNSSs with multi frequency data, many more ionosphere-sensing combinations of different precision can be formed as input of ionospheric modelling. We present the general way of interpreting such combinations through an application of $\mathcal{S}$-system theory and address how their precision propagates into that of the unbiased TEC solution. Presenting the data relevant to TEC determination, we propose the usage of an array of GNSS antennas to improve the TEC precision and to expedite the rather long observational time-span required for high-precision TEC determination.

Keywords: singularity-system theory, Global Navigation Satellite Systems (GNSS), total electron content (TEC), ionospheric estimability, array-based setup

1. INTRODUCTION

The GNSS carrier-phase and code data have proven to be valuable sources of measuring the Earth's ionospheric total electron content (TEC) (see, e.g., *Sardon et al., 1994*; *Schaer et al., 1995*; *Sardon and Zarraoa, 1997*; *Mannucci et al., 1998*; *Hernández-Pajares et al., 2005*; *Ciraolo et al., 2007*; *Brunini and Azpilicueta, 2009*; *Yue et al., 2014*). Due to the presence of the unknown carrier-phase ambiguities and code instrumental biases however, the observed ionospheric delays, experienced on these data, do not represent the unbiased slant TEC. In order to retrieve the unbiased TEC, one therefore has to take recourse to an external ionospheric model for which GNSS derived combinations of the ionospheric delays and ambiguity/code biases serve as input. In case of GPS dual-frequency data, the well-known geometry-free phase and code combinations take the role of such ionosphere sensing combinations (*Schaer, 1999*). Each set of such combinations presents its own interpretation and precision. In the light of the development of new GNSSs with multi frequency data, many more ionosphere-sensing combinations of different precision can be formed as input of ionospheric modelling. It is the goal of the

present contribution to address how such combinations should be interpreted and why one should not base one's precision analysis of TEC on that of the ionosphere-sensing combinations. As shown by *Khodabandeh and Teunissen (2016)*, one can rigorously remove the underlying rank-deficiency of the GNSS observations for the purpose of array-based TEC estimation. The present contribution is a continuation of (ibid) where we review the singularity system ($\mathcal{S}$-system) theory (*Baarda, 1973*; *Teunissen, 1985*) through an illustrative example and apply the theory to the rank-deficient GNSS observation equations via three different $\mathcal{S}$-systems. The intrinsic lack of information content in the GNSS data is characterized by identifying the corresponding model's null-space. Choosing three different $\mathcal{S}$-systems, it is shown that the ionosphere-sensing combinations are nothing else, but estimable versions of the slant ionospheric delays. We show the dependency of their precision on the choice of $\mathcal{S}$-system and address how their precision propagates into that of the unbiased TEC solution. By presenting the GNSS data of relevance for TEC determination, we propose the usage of an array of GNSS antennas to improve the TEC precision and to expedite the rather long observational time-span required for high-precision TEC determination.

We make use of the following notation: The expectation, covariance and dispersion operators are denoted as $E(\cdot)$, $C(\cdot,\cdot)$ and $D(\cdot)$, respectively. The capital Q is reserved for variance matrices. Thus $C(\boldsymbol{y},\boldsymbol{y}) = D(\boldsymbol{y}) = \mathbf{Q}_{yy}$, with $\boldsymbol{y}$ being a random vector. The identity matrix of order n is denoted by $\mathbf{I}_n$. The n-vector of ones (the summation vector) is denoted by $\boldsymbol{e}_n$. Wherever the subscript n is omitted, the order of $\mathbf{I}$ and the size of $\boldsymbol{e}$ are meant to be equal to the number of GNSS frequencies f. Thus $\mathbf{I} = \mathbf{I}_f$ and $\boldsymbol{e} = \boldsymbol{e}_f$. Frequent use of the matrix Kronecker product $\otimes$ (*Henderson et al., 1983*) is made for the vectorial representation. The range-space (column-space) of matrix $\mathbf{A} \in \mathbb{R}^{m\times n}$ is denoted by $\mathcal{R}(\mathbf{A})$. The matrix $\mathbf{A}^{\perp}$ denotes a basis matrix where $\mathcal{R}(\mathbf{A}^{\perp})$ is the orthogonal complement to $\mathcal{R}(\mathbf{A})$, thus $\mathbf{A}^{\mathrm{T}}\mathbf{A}^{\perp} = \mathbf{0}$ and $\mathcal{R}(\mathbf{A}) \oplus \mathcal{R}(\mathbf{A}^{\perp}) = \mathbb{R}^m$, with the 'direct sum' being symbolized by $\oplus$.

2. RANK-DEFICIENT LINEAR MODELS

As our point of departure, we commence with the linear model

$$E(\boldsymbol{y}) = \mathbf{A}\boldsymbol{x}\ , \quad \mathbf{A} \in \mathbb{R}^{m\times n}, \quad D(\boldsymbol{y}) = \mathbf{Q}_{yy}\ , \tag{1}$$

where the observation and parameter vectors are denoted by $\boldsymbol{y}$ and $\boldsymbol{x}$, respectively. The variance matrix $\mathbf{Q}_{yy}$ is assumed positive-definite, while the design matrix $\mathbf{A}$ can be rank-deficient. By rank-deficient, we mean some of the columns of $\mathbf{A}$ are linearly dependent so that not all the elements of $\boldsymbol{x}$ can be unbiasedly determined, given the information content in $\boldsymbol{y}$.

To better appreciate the rank-deficiency concept, let us first consider a two-dimensional example (i.e. $n = 2$) by setting $\mathbf{A} = [2, -1]$ and $\boldsymbol{x} = [x_1, x_2]^{\mathrm{T}}$. Thus one single observation $\boldsymbol{y}$ serves to determine the two unknowns x_1 and x_2. As at most one unknown can be determined, the linear model $E(\boldsymbol{y}) = 2x_1 - x_2$ must be expressed by at most one single parameter. Many (in fact infinite) such expressions exist. They can be represented by

$$E(\boldsymbol{y}) = 2x_1 - x_2 = (2a - b)\frac{2x_1 - x_2}{2a - b} = (2a - b)w = 2\underbrace{aw}_{x_{1;S}} - \underbrace{bw}_{x_{2;S}}, \tag{2}$$

with

$$w = \frac{2x_1 - x_2}{2a - b}, \quad b \neq 2a .$$

Reducing the two unknowns x_1 and x_2 to one unknown w, the above model is now solvable for w. As this parameter can be estimated through Eq. (2), any function of w is referred to as an estimable parameter. For instance, the estimable version of the parameter vector $\boldsymbol{x}$ is symbolized by

$$\boldsymbol{x}_{;S} = \left[x_{1;S}, x_{2;S} \right]^{\mathrm{T}}$$

and given by

$$\boldsymbol{x}_{;S} = \mathbf{S}w \quad \text{with} \quad \mathbf{S} = \begin{bmatrix} a \\ b \end{bmatrix} . \tag{3}$$

Equations (3) show that the estimable versions of $\boldsymbol{x}$ are all formed by w. The way they are formed is driven by the choice of a and b. Each choice leads to its own solvable model (2) with a 'distinct' vector $\mathbf{S}$. It is indeed the choice of this vector that enables us to transform the rank-deficient model $E(\boldsymbol{y}) = 2x_1 - x_2$ into the solvable model $E(\boldsymbol{y}) = (2a - b)w$. By choosing $\mathbf{S}$, we define our '$\mathcal{S}$-system' to pick the particular solution $\boldsymbol{x}_{;S}$ out of infinite solutions for $\boldsymbol{x}$. To see this, consider the representation linking the particular solution $\boldsymbol{x}_{;S}$ to $\boldsymbol{x}$ as follows

$$\boldsymbol{x} = \boldsymbol{x}_{;S} + \mathbf{V}\frac{ax_2 - bx_1}{2a - b}, \quad \text{with } \mathbf{V} = \begin{bmatrix} 1 \\ 2 \end{bmatrix} . \tag{4}$$

Since the vectors $\mathbf{S}$ and $\mathbf{V}$ are linearly independent ($b \neq 2a$), their range-spaces, i.e. $\mathcal{R}(\mathbf{S})$ and $\mathcal{R}(\mathbf{V})$, span the whole parameter space $\mathbb{R}^2$ (see Fig. 1). Thus the parameter vector $\boldsymbol{x}$ can always be expressed as a linear combination of $\mathbf{S}$ and $\mathbf{V}$. The vector $\mathbf{V}$ has the

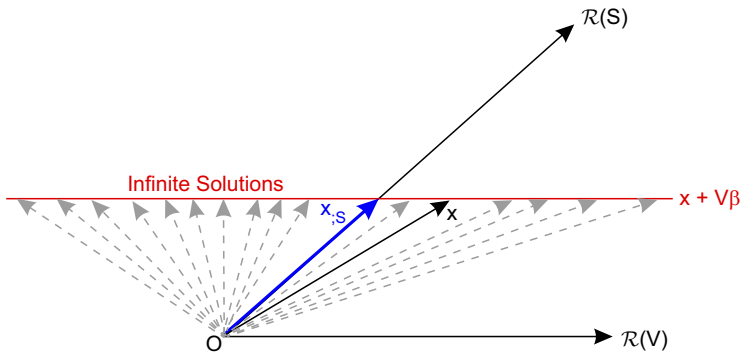

Fig. 1. Geometrical illustration of the infinite solutions of the rank-deficient model given by Eq. (1). All the solutions (grey dashed lines) are mapped versions of one another along the null-space $\mathcal{R}(\mathbf{V})$. By choosing the $\mathcal{S}$-system $\mathcal{R}(\mathbf{S})$ complementary to $\mathcal{R}(\mathbf{V})$, one picks the particular solution $\boldsymbol{x}_{;S}$ out of infinite solutions for $\boldsymbol{x}$.

property of nullifying the design matrix **A**, that is, $\mathbf{AV}=0$. With this, substitution of Eq. (4) into $E(\boldsymbol{y})=\mathbf{A}\boldsymbol{x}$ gives

$$E(\boldsymbol{y})=\mathbf{A}\boldsymbol{x}=\mathbf{A}\boldsymbol{x}_{;S}=(\mathbf{AS})w\ . \tag{5}$$

As the above model is solvable for w, the columns of **AS** are linearly independent, representing a new full-rank design matrix. According to Eq. (5), one can choose one's $\mathcal{S}$-system **S**, complement to **V**, to define one's full-rank design matrix **AS**. The notion presented for the above two-dimensional example ($n=2$) can carry over to the general case. The role of the 'vectors' **S** and **V** are then taken by their 'matrix' counterparts, extending the single parameter w to a vector. The general formulation of $\mathcal{S}$-system theory was introduced and developed by *Baarda (1973)* and *Teunissen (1985)*. The representation of a full-rank model defined by an $\mathcal{S}$-system is recapitulated below.

Definition: (full-rank model defined by an $\mathcal{S}$-system) Let **V** be a basis matrix spanning the null-space of the design matrix **A** in Eq. (1), i.e.

$$\mathcal{R}(\mathbf{V})=\left\{\boldsymbol{v}\in\mathbb{R}^n\,\middle|\,\mathbf{A}v=0\right\}\ . \tag{6}$$

By choosing the arbitrary basis matrix **S** where its range-space is complementary to that of **V**, i.e.

$$\mathcal{R}(\mathbf{S})\oplus\mathcal{R}(\mathbf{V})=\mathbb{R}^n \tag{7}$$

a full-rank version of Eq. (1) is formed by **S** as follows

$$E(\boldsymbol{y}) = (\mathbf{AS})w \;, \quad \mathbf{AS} = \mathbb{R}^{m \times r} \;, \quad D(\boldsymbol{y}) = \mathbf{Q}_{yy} \;, \tag{8}$$

With r being the rank of $\mathbf{A}$ and the parameter vector $\boldsymbol{w}$ containing estimable functions of $\boldsymbol{x}$. The corresponding estimable version of $\boldsymbol{x}$ is given as $\boldsymbol{x}_{;S} = \mathbf{S}w$.

According to the above definition, the solution of $\boldsymbol{x}_{;S}$ as well as its precision depend on the choice of $\mathbf{S}$. The variance matrix of the least-squares solution of $\boldsymbol{x}_{;S}$ is obtained as follows

$$\mathbf{Q}_{\hat{x}_{;S}\hat{x}_{;S}} = \mathbf{S}\left(\mathbf{S}^{\mathrm{T}}\mathbf{A}^{\mathrm{T}}\mathbf{Q}_{yy}^{-1}\mathbf{AS}\right)^{-1}\mathbf{S}^{\mathrm{T}} . \tag{9}$$

With regard to Eq. (3), application to the two-dimensional example ($\mathbf{Q}_{yy}$ replaced by the variance σ_y^2) gives

$$\mathbf{Q}_{\hat{x}_{;S}\hat{x}_{;S}} = \frac{\sigma_y^2}{(2a-b)^2}\begin{bmatrix} a \\ b \end{bmatrix}\begin{bmatrix} a \\ b \end{bmatrix}^{\mathrm{T}} . \tag{10}$$

Thus different choices of a and b lead to estimable parameters of different precision. One can, for instance, set these values such that the 'trace' of $\mathbf{Q}_{\hat{x}_{;S}\hat{x}_{;S}}$ gets minimized. Taking the trace of Eq. (10) yields

$$\mathrm{tr}\left(\mathbf{Q}_{\hat{x}_{;S}\hat{x}_{;S}}\right) = \frac{a^2+b^2}{(2a-b)^2}\sigma_y^2 = \frac{1}{5\cos^2\theta}\sigma_y^2 \geq \frac{1}{5}\sigma_y^2 \;, \tag{11}$$

with θ being the angle between the vectors $[a, b]^{\mathrm{T}}$ and $[2, -1]^{\mathrm{T}}$. One can choose the vector $\mathbf{S} = [a, b]^{\mathrm{T}}$ to be parallel with $[2, -1]^{\mathrm{T}}$ (i.e. $\theta = 0$), thereby achieving the minimum-trace variance matrix among all possible estimable solutions $\hat{\boldsymbol{x}}_{;S}$. As the vector $[2, -1]^{\mathrm{T}}$ is 'orthogonal' to $\mathbf{V}$ given in Eq. (4), such an $\mathcal{S}$-system follows by choosing

$$\mathbf{S} = \mathbf{V}^{\perp}, \quad \text{with} \quad \mathbf{V}^{\mathrm{T}}\mathbf{V}^{\perp} = 0 \;. \tag{12}$$

Such a choice of $\mathcal{S}$-system also minimizes the 'length' of the 1σ confidence interval of $\hat{\boldsymbol{x}}_{;S}$. Using the unit vector of $\mathbf{S}$ as

$$\boldsymbol{u} = \frac{1}{\sqrt{a^2+b^2}}\begin{bmatrix} a \\ b \end{bmatrix} , \tag{13}$$

the stated length is computed by

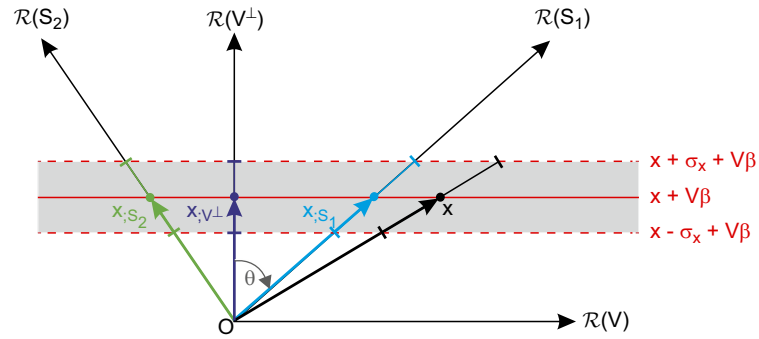

Fig. 2. Precision dependency of the estimable parameters $\boldsymbol{x}_{;S_1}$, $\boldsymbol{x}_{;S_2}$ and $\boldsymbol{x}_{;V^\perp}$ on their choice of $\mathcal{S}$-system. Their corresponding 1σ confidence intervals are symbolized by error bars within the grey area. The smaller the angle between the range-spaces $\mathcal{R}(\mathbf{S})$ and $\mathcal{R}(\mathbf{V})$, the larger the variance becomes. With the choice of $\mathbf{S} = \mathbf{V}^\perp$, the variance attains its minimum.

$$\sqrt{\boldsymbol{u}^{\mathrm{T}}\mathbf{Q}_{\hat{x}_{;S}\,\hat{x}_{;S}}\boldsymbol{u}} = \frac{\sqrt{a^2+b^2}}{|2a-b|}\sigma_y = \frac{1}{\sqrt{5}|\cos\theta|}\sigma_y \ . \tag{14}$$

As shown in Fig. 2, the smaller the angle between the range-spaces $\mathcal{R}(\mathbf{S})$ and $\mathcal{R}(\mathbf{V}^\perp)$, the smaller the above length becomes. When the stated angle θ becomes 0, i.e. $\mathcal{R}(\mathbf{S}) = \mathcal{R}(\mathbf{V}^\perp)$, the length attains its minimum. The same conclusion can be made for the general case.

Lemma 1 (Minimum-trace variance matrix): Let $\mathbf{V}^\perp$ be a basis matrix where its range-space is the orthogonal complement to $\mathcal{R}(\mathbf{V})$. Then the choice of $\mathbf{V}^\perp$ as the $\mathcal{S}$-system of Eq. (1) leads to the minimum-trace variance matrix $\mathbf{Q}_{\hat{x}_{;S}\,\hat{x}_{;S}}$ among all possible $\mathcal{S}$-systems, that is

$$\mathrm{tr}\left(\mathbf{Q}_{\hat{x}_{;V^\perp}\,\hat{x}_{;V^\perp}}\right) \le \mathrm{tr}\left(\mathbf{Q}_{\hat{x}_{;S}\,\hat{x}_{;S}}\right) \tag{15}$$

for all $\mathbf{S}$ satisfying Eq. (7). Proof is presented in the Appendix.

Given the outcome of Lemma 1, one may be tempted to prefer the choice of $\mathbf{S} = \mathbf{V}^\perp$ to other $\mathcal{S}$-systems as it ensures the minimum-trace variance matrix of $\hat{\boldsymbol{x}}_{;S}$. It should, however, be remarked that each $\mathcal{S}$-system represents its own estimable parameters (cf. Eq.(3)). Consider, for instance, the three distinct choices $\mathbf{S}_1$, $\mathbf{S}_2$ and $\mathbf{V}^\perp$ shown in Fig. 2. Since

$$\boldsymbol{x}_{;S_1} \neq \boldsymbol{x}_{;S_2} \neq \boldsymbol{x}_{;V^\perp}\,, \tag{16}$$

it is evident that neither their solutions nor their precision are necessarily the same. Although the solution $\hat{\boldsymbol{x}}_{;V^\perp}$ has the minimum-trace variance matrix, it cannot be directly compared with the solution $\hat{\boldsymbol{x}}_{;S_1}$ as both describe two different quantities. In the following, further insights are provided through applying three $\mathcal{S}$-systems to the GNSS single-antenna observation equations.

3. GNSS FULL-RANK MODELS VIA THREE S-SYSTEMS

3.1. Single-antenna linear model

Let $\varphi_{r,j}^{s}$ and $p_{r,j}^{s}$ be, respectively, the phase and code observations of satellite s ($s = 1, \ldots, m$) on frequency band f_j ($j = 1, \ldots, f$) that are collected by the single antenna r. The corresponding phase observation vector is defined as $\boldsymbol{\varphi}_r = \left[\, \boldsymbol{\varphi}_{r,1}^{\mathrm{T}}, \ldots, \boldsymbol{\varphi}_{r,f}^{\mathrm{T}} \,\right]^{\mathrm{T}} \in \mathbb{R}^{fm}$, where $\boldsymbol{\varphi}_{r,j} = \left[\, \varphi_{r,j}^{1}, \ldots, \varphi_{r,j}^{m} \,\right]^{\mathrm{T}} \in \mathbb{R}^{m}$. With a likewise definition for the code observation vector $\boldsymbol{p}_r \in \mathbb{R}^{fm}$, the GNSS single-antenna linear model reads (*Khodabandeh and Teunissen, 2015a*)

$$E\left(\begin{bmatrix} \boldsymbol{\varphi}_r \\ \boldsymbol{p}_r \end{bmatrix}\right) = \left(\begin{bmatrix} -\boldsymbol{\mu}, \boldsymbol{e} \\ +\boldsymbol{\mu}, \boldsymbol{e} \end{bmatrix} \otimes \mathbf{I}_m\right)\begin{bmatrix} \boldsymbol{i}_r \\ \boldsymbol{p}_r \end{bmatrix} + \begin{bmatrix} \boldsymbol{a}_r \\ \boldsymbol{d}_r \end{bmatrix}, \quad D\left(\begin{bmatrix} \boldsymbol{\varphi}_r \\ \boldsymbol{p}_r \end{bmatrix}\right) = \sigma_p^2 \begin{bmatrix} \varepsilon\mathbf{I}, 0 \\ 0, \mathbf{I} \end{bmatrix} \otimes \mathbf{C}\,, \tag{17}$$

where the m-vector $\boldsymbol{i}_r$ contains the (first-order) slant ionospheric delays i_r^s ($s = 1, \ldots, m$) experienced on the first frequency. The corresponding frequency-dependent coefficients $\mu_j = f_1^2 / f_j^2$ ($j = 1, \ldots, f$) form the f-vector $\boldsymbol{\mu}$. The nondispersive delays including the geometric ranges, clocks and the tropospheric delays are collected in the m-vector $\boldsymbol{\rho}_r$. The real-valued ambiguities $a_{r,j}^{s}$ are expressed in units of range and collected in $\boldsymbol{a}_r = \left[\, \boldsymbol{a}_{r,1}^{\mathrm{T}}, \ldots, \boldsymbol{a}_{r,f}^{\mathrm{T}} \,\right]^{\mathrm{T}} \in \mathbb{R}^{fm}$, with $\boldsymbol{a}_{r,j} = \left[\, a_{r,j}^{1}, \ldots, a_{r,j}^{m} \,\right]^{\mathrm{T}}$. Likewise, the vector $\boldsymbol{d}_r \in \mathbb{R}^{fm}$ contains the lumped terms $d_{r,j}^{s} = d_{r,j} - d_{,j}^{s}$, where $d_{r,j}$ and $d_{,j}^{s}$ denote the receiver and satellite code biases, respectively.

The second formula of Eq. (17) structures the variance matrix of the observations. The $m \times m$ diagonal matrix $\mathbf{C}$ contains the satellite elevation-dependent co-factors. This matrix changes in time as the satellites' elevation changes. The zenith-referenced variance of the code data is denoted by σ_p^2, whereas ε denotes the phase-to-code variance ratio. Since the precision of the phase data is almost two orders of magnitude better than that of the code

data, the stated ratio ε is set to 0.0001 in most GNSS applications. With such precision diversity - as will be shown later - estimable parameters of various precision levels are formed.

3.2. Null-space of the single-antenna model

The first formula of Eq. (17) represents an underdetermined system of equations, i.e. $2f$ equations with $2f + 2$ unknowns per satellite. Thus the model is solvable for at most $2fm$ unknowns, leaving $2m$ unknowns inestimable due to the lack of information content in the model. This lack of information is characterized through the null-space of the model. To form a null-space basis matrix, we define the parameter vector $\boldsymbol{x} = \left[\boldsymbol{i}_r^{\mathrm{T}}, \boldsymbol{\rho}_r^{\mathrm{T}}, \boldsymbol{a}_r^{\mathrm{T}}, \boldsymbol{d}_r^{\mathrm{T}} \right]^{\mathrm{T}}$, giving rise to the following design matrix of Eq. (17)

$$\mathbf{A} = \begin{bmatrix} -\boldsymbol{\mu}, \boldsymbol{e}, \mathbf{I}, 0 \\ +\boldsymbol{\mu}, \boldsymbol{e}, 0, \mathbf{I} \end{bmatrix} \otimes \mathbf{I}_m \ . \tag{18}$$

The above matrix is nullified by the basis matrix

$$\mathbf{V} = \begin{bmatrix} 1, 0 \\ 0, 1 \\ +\boldsymbol{\mu}, -\boldsymbol{e} \\ -\boldsymbol{\mu}, -\boldsymbol{e} \end{bmatrix} \otimes \mathbf{I}_m \ . \tag{19}$$

Now that the null-space basis matrix $\mathbf{V}$ is structured, we are in a position to choose any basis matrix $\mathbf{S}$ satisfying the condition given by Eq. (7), thereby forming the corresponding full-rank model. In the following, three examples of $\mathbf{S}$ are presented. In each example, we parametrize $\boldsymbol{x}$ in terms of the $\boldsymbol{w}$ and $\boldsymbol{\beta}$ parameters as follows (cf. Eq. (4))

$$\boldsymbol{x} = \left[\mathbf{S}, \mathbf{V} \right] \begin{bmatrix} \boldsymbol{w} \\ \boldsymbol{\beta} \end{bmatrix} \quad \Leftrightarrow \quad \left[\mathbf{S}, \mathbf{V} \right]^{-1} \boldsymbol{x} = \begin{bmatrix} \boldsymbol{w} \\ \boldsymbol{\beta} \end{bmatrix} , \tag{20}$$

where the parameter vector $\boldsymbol{\beta}$ stands for the inestimable components of $\boldsymbol{x}$. The estimable version of $\boldsymbol{x}$ would then follow from

$$\boldsymbol{x}_{;S} = \boldsymbol{x} - \mathbf{V}\boldsymbol{\beta} = \mathbf{S}\boldsymbol{w} . \tag{21}$$

3.3. S-system S_1: code-leveled ionospheric delays

We first focus on the observation equations of the code data $\boldsymbol{p}_r$. The idea is to have the code-only system of equations solvable as well. For that, we choose our $\mathcal{S}$-system $\mathbf{S}_1$ such that the columns of $\mathbf{AS}_1$ corresponding to the code biases on the first two frequencies $j = 1, 2$, i.e. $d_{r,1}^s$ and $d_{r,2}^s$ ($s = 1, \ldots, m$), get eliminated. This choice corresponds to forming the following basis matrix

$$\mathbf{S}_1 = \begin{bmatrix} 1 & 0 & 0 & 0 \\ 0 & 1 & 0 & 0 \\ 0 & 0 & \mathbf{I} & 0 \\ 0 & 0 & 0 & \mathbf{E} \end{bmatrix} \otimes \mathbf{I}_m \ , \tag{22}$$

where the $f \times (f-2)$ matrix $\mathbf{E}$ is formed by eliminating the first two columns of $\mathbf{I}$. Upon this choice, an application of the second expression of Eq. (20) results in $\boldsymbol{\beta} \to -\left[\left(\boldsymbol{\mu}_{GF}^{\mathrm{T}} \boldsymbol{d}_r \right)^{\mathrm{T}}, \left(\boldsymbol{\mu}_{IF}^{\mathrm{T}} \boldsymbol{d}_r \right)^{\mathrm{T}} \right]^{\mathrm{T}}$, thereby reducing the general parametrization of Eq. (21) to

$$\begin{bmatrix} \boldsymbol{i}_{r;S_1} \\ \boldsymbol{\rho}_{r;S_1} \\ \boldsymbol{a}_{r;S_1} \\ \boldsymbol{d}_{r;S_1} \end{bmatrix} = \begin{bmatrix} \boldsymbol{i}_r \\ \boldsymbol{\rho}_r \\ \boldsymbol{a}_r \\ \boldsymbol{d}_r \end{bmatrix} - \mathbf{V} \begin{bmatrix} -\boldsymbol{\mu}_{GF}^{\mathrm{T}} \boldsymbol{d}_r \\ -\boldsymbol{\mu}_{IF}^{\mathrm{T}} \boldsymbol{d}_r \end{bmatrix} , \tag{23}$$

in which the 'geometry-free' (GF) and 'ionosphere-free' (IF) combinations are, respectively, defined as

$$\boldsymbol{\mu}_{GF} = \frac{1}{\mu_2 - \mu_1} [-1, +1, 0, \ldots, 0]^{\mathrm{T}}, \quad \boldsymbol{\mu}_{IF} = \frac{1}{\mu_2 - \mu_1} [\mu_2, -\mu_1, 0, \ldots, 0]^{\mathrm{T}} . \tag{24}$$

With regard to $\boldsymbol{x}_{;S_1} = \mathbf{S}_1 \boldsymbol{w}$ and Eq. (23), the $\boldsymbol{w}$ parameters read

$$\boldsymbol{w} \to \left[\boldsymbol{i}_{r;S_1}^{\mathrm{T}}, \boldsymbol{\rho}_{r;S_1}^{\mathrm{T}}, \boldsymbol{a}_{r;S_1}^{\mathrm{T}}, \tilde{\boldsymbol{d}}_{r;S_1}^{\mathrm{T}} \right]^{\mathrm{T}} . \tag{25}$$

The estimable vector $\tilde{\boldsymbol{d}}_{r;S_1}$ is structured by removing the first 2*m* elements of the estimable code biases $\boldsymbol{d}_{r;S_1}$. Substitution of Eq. (23) into Eq. (17), together with $\mathbf{AV} = 0$, provides us with the full-rank model

$$E\left(\begin{bmatrix} \boldsymbol{\varphi}_r \\ \boldsymbol{p}_r \end{bmatrix} \right) = \left(\begin{bmatrix} -\boldsymbol{\mu}, \boldsymbol{e} \\ +\boldsymbol{\mu}, \boldsymbol{e} \end{bmatrix} \otimes \mathbf{I}_m \right) \begin{bmatrix} \boldsymbol{i}_{r;S_1} \\ \boldsymbol{\rho}_{r;S_1} \end{bmatrix} + \left(\begin{bmatrix} \mathbf{I}, 0 \\ 0, \mathbf{E} \end{bmatrix} \times \mathbf{I}_m \right) \begin{bmatrix} \boldsymbol{a}_{r;S_1} \\ \tilde{\boldsymbol{d}}_{r;S_1} \end{bmatrix} . \tag{26}$$

The above model is now solvable as it is expressed as an invertible system of 2*f* equations with 2*f* unknowns per satellite. Since the columns corresponding to the code biases $d_{r,1}^s$ and $d_{r,2}^s$ (s = 1, …, m) were eliminated, the code-only part of Eq. (26), i.e.,

$$E(\boldsymbol{p}_r) = \left([+\boldsymbol{\mu}, \boldsymbol{e}] \otimes \mathbf{I}_m \right) \begin{bmatrix} \boldsymbol{i}_{r;S_1} \\ \boldsymbol{\rho}_{r;S_1} \end{bmatrix} + \left(\mathbf{E} \otimes \mathbf{I}_m \right) \tilde{\boldsymbol{d}}_{r;S_1} \tag{27}$$

also represents a solvable model. It links the *fm* observations $\boldsymbol{p}_r$ to *fm* unknowns $\boldsymbol{i}_{r;S_1}$ (of size *m*), $\boldsymbol{\rho}_{r;S_1}$ (of size *m*) and $\tilde{\boldsymbol{d}}_{r;S_1}$ (of size $(f-2)m$).

With Eq. (26), the *fm* precise phase data φ_r are all reserved for the *fm* estimable ambiguities $\boldsymbol{a}_{r;S_1}$. As a consequence, the rather poorly-precise code data $\boldsymbol{p}_r$ govern the solutions of the estimable parameters involved in Eq. (26), including the estimable slant ionospheric delays $\boldsymbol{i}_{r;S_1}$. As these parameters are of particular interest for the GNSS ionospheric sensing, let us have a closer look at their interpretation given in Eq. (23). The first row of Eq. (23) gives

$$\boldsymbol{i}_{r;S_1} = \boldsymbol{i}_r + \boldsymbol{\mu}_{GF}^{\mathrm{T}} \boldsymbol{d}_r \quad . \tag{28}$$

Thus the estimable parameters $\boldsymbol{i}_{r;S_1}$ consist of the unbiased ionospheric delays $\boldsymbol{i}_r$ that are biased by the GF combinations of the code biases, i.e. $\boldsymbol{\mu}_{GF}^{\mathrm{T}} \boldsymbol{d}_r$. The code bias combination $\boldsymbol{\mu}_{GF}^{\mathrm{T}} \boldsymbol{d}_r$ is referred to as the 'differential code bias' (DCB) which is also known as the 'inter-frequency bias' (*Schaer, 1999*). Since this bias is specified by its corresponding satellite, the corresponding technique of retrieving the slant unbiased delays $\boldsymbol{i}_r$ is therefore known as the 'satellite-by-satellite' calibration technique (*Brunini and Azpilicueta, 2009*). Given an external ionospheric model, the so-called code-leveled ionospheric delays $\boldsymbol{i}_{r;S_1}$ serve as input to retrieve $\boldsymbol{i}_r$. With respect to our earlier remark on the code-driven precision of $\boldsymbol{i}_{r;S_1}$, it is therefore of importance to understand how this poor precision propagates into that of the solution $\hat{\boldsymbol{i}}_{r;S_1}$. Before addressing this point, we present two other estimable forms of the ionospheric delays. They are more precise than $\hat{\boldsymbol{i}}_{r;S_1}$ and can also serve as input of the ionospheric retrieval.

3.4. S-system S_2: phase-leveled ionospheric delays

We now turn our attention to the observation equations of the phase data $\boldsymbol{\varphi}_r$, aiming to have the phase-only system of equations solvable as well. Instead of the code biases, the $\mathcal{S}$-system $\mathbf{S}_2$ is chosen such that the columns of $\mathbf{AS}_2$ corresponding to the ambiguities on the first two frequencies $j = 1, 2$, i.e. $a_{r,1}^s$ and $a_{r,2}^s$ ($s = 1, \ldots, m$), get eliminated. This choice is realized by the following basis matrix

$$\mathbf{S}_2 = \begin{bmatrix} 1 & 0 & 0 & 0 \\ 0 & 1 & 0 & 0 \\ 0 & 0 & \mathbf{E} & 0 \\ 0 & 0 & 0 & \mathbf{I} \end{bmatrix} \otimes \mathbf{I}_m \quad . \tag{29}$$

Compare the above choice with Eq. (22). The coefficient matrix **E** is now assigned to the ambiguities rather than the code biases. With this choice, an application of the second expression of Eq. (20) yields $\boldsymbol{\beta} \to \left[\left(\boldsymbol{\mu}_{GF}^{\mathrm{T}} \boldsymbol{a}_r \right)^{\mathrm{T}} , -\left(\boldsymbol{\mu}_{IF}^{\mathrm{T}} \boldsymbol{a}_r \right)^{\mathrm{T}} \right]^{\mathrm{T}}$. The parametrization of Eq. (21) is reduced to

$$\begin{bmatrix} \boldsymbol{i}_{r;S_2} \\ \boldsymbol{\rho}_{r;S_2} \\ \boldsymbol{a}_{r;S_2} \\ \boldsymbol{d}_{r;S_2} \end{bmatrix} = \begin{bmatrix} \boldsymbol{i}_r \\ \boldsymbol{\rho}_r \\ \boldsymbol{a}_r \\ \boldsymbol{d}_r \end{bmatrix} - \mathbf{V} \begin{bmatrix} +\boldsymbol{\mu}_{GF}^{\mathrm{T}} \boldsymbol{a}_r \\ -\boldsymbol{\mu}_{IF}^{\mathrm{T}} \boldsymbol{a}_r \end{bmatrix} . \tag{30}$$

With regard to $\boldsymbol{x}_{;S_2} = \mathbf{S}_2 \boldsymbol{w}$ and Eq. (30), the *w* is determined by (compare with Eq. (25))

$$\boldsymbol{w} \to \left[\boldsymbol{i}_{r;S_2}^{\mathrm{T}} , \boldsymbol{\rho}_{r;S_2}^{\mathrm{T}} , \tilde{\boldsymbol{a}}_{r;S_2}^{\mathrm{T}} , \boldsymbol{d}_{r;S_2}^{\mathrm{T}} \right]^{\mathrm{T}} . \tag{31}$$

The estimable vector $\tilde{\boldsymbol{a}}_{r;S_2}$ is formed by removing the first 2*m* elements of the estimable ambiguities $\boldsymbol{a}_{r;S_2}$. Substitution of Eq. (30) into Eq. (17) gives another full-rank single-antenna model, that is

$$E\left(\begin{bmatrix} \boldsymbol{\varphi}_r \\ \boldsymbol{p}_r \end{bmatrix} \right) = \left(\begin{bmatrix} -\boldsymbol{\mu}, \boldsymbol{e} \\ +\boldsymbol{\mu}, \boldsymbol{e} \end{bmatrix} \otimes \mathbf{I}_m \right) \begin{bmatrix} \boldsymbol{i}_{r;S_2} \\ \boldsymbol{\rho}_{r;S_2} \end{bmatrix} + \left(\begin{bmatrix} \mathbf{E}, 0 \\ 0, \mathbf{I} \end{bmatrix} \times \mathbf{I}_m \right) \begin{bmatrix} \tilde{\boldsymbol{a}}_{r;S_2} \\ \boldsymbol{d}_{r;S_2} \end{bmatrix} . \tag{32}$$

Similar to Eq. (26), this model also links 2*fm* observations to 2*fm* unknowns. Only the roles of $\boldsymbol{a}_{r;S_1}$ and $\tilde{\boldsymbol{d}}_{r;S_1}$ are interchanged by those of $\boldsymbol{d}_{r;S_2}$ and $\tilde{\boldsymbol{a}}_{r;S_2}$, respectively. Such a minor change leads the precision of some of the involved estimable parameters to be driven by the very-precise phase data $\boldsymbol{\varphi}_r$. To see this, consider the phase-only part of Eq. (32)

$$E\left(\boldsymbol{\varphi}_r \right) = \left(\left[-\boldsymbol{\mu}, \boldsymbol{e} \right] \otimes \mathbf{I}_m \right) \begin{bmatrix} \boldsymbol{i}_{r;S_2} \\ \boldsymbol{\rho}_{r;S_2} \end{bmatrix} + \left(\mathbf{E} \otimes \mathbf{I}_m \right) \tilde{\boldsymbol{a}}_{r;S_2} , \tag{33}$$

which is a solvable model. Since the *fm* code data $\boldsymbol{p}_r$ are all reserved for the *fm* estimable code biases $\boldsymbol{d}_{r;S_2}$ in Eq. (32), the estimable parameters $\boldsymbol{i}_{r;S_2}$, $\boldsymbol{\rho}_{r;S_2}$ and $\tilde{\boldsymbol{a}}_{r;S_2}$ are obtained by the phase-only model (33), thus having the phase level of precision. The interpretation of the corresponding phase-driven ionospheric delays $\boldsymbol{i}_{r;S_2}$ follows from the first row of Eq. (30) as

$$\boldsymbol{i}_{r;S_2} = \boldsymbol{i}_r - \boldsymbol{\mu}_{GF}^{\mathrm{T}} \boldsymbol{a}_r . \tag{34}$$

Thus the phase-leveled ionospheric delays $\boldsymbol{i}_{r;S_2}$ consist of the unbiased ionospheric delays $\boldsymbol{i}_r$ that are biased by the GF combinations of the ambiguities, i.e. $\boldsymbol{\mu}_{GF}^{\mathrm{T}}\boldsymbol{a}_r$. Since the ambiguities are specified by their satellite' arcs, the corresponding technique of retrieving the slant unbiased delays $\boldsymbol{i}_r$ is therefore known as the 'arc by-arc' calibration technique (*Brunini and Azpilicueta, 2009*).

3.5. S-system $\mathbf{V}^{\perp}$: minimum-trace variance matrix

Motivated by the outcome of Lemma 1, one may prefer to work with the full-rank single-antenna model defined by the choice of $\mathbf{S} = \mathbf{V}^{\perp}$. An orthogonal complement basis matrix to $\mathbf{V}$, introduced in Eq. (19), is given by

$$\mathbf{V}^{\perp} = \begin{bmatrix} -\boldsymbol{\mu}^{\mathrm{T}}, +\boldsymbol{\mu}^{\mathrm{T}} \\ \boldsymbol{e}^{\mathrm{T}}, \boldsymbol{e}^{\mathrm{T}} \\ \mathbf{I}, 0 \\ 0, \mathbf{I} \end{bmatrix} \otimes \mathbf{I}_m \ . \tag{35}$$

With this choice of $\mathcal{S}$-system, the $\boldsymbol{\beta}$ parameters follow from the second expression of Eq. (20) as

$$\begin{aligned} \boldsymbol{\beta}_1 &= \frac{1}{1+2\boldsymbol{\mu}^{\mathrm{T}}\boldsymbol{\mu}}\Big[\boldsymbol{i}_r - \Big(\boldsymbol{\mu}^{\mathrm{T}} \otimes \mathbf{I}_m\Big)\big(\boldsymbol{d}_r - \boldsymbol{a}_r\big)\Big], \\ \boldsymbol{\beta}_2 &= \frac{1}{1+2\boldsymbol{e}^{\mathrm{T}}\boldsymbol{e}}\Big[\boldsymbol{\rho}_r - \Big(\boldsymbol{e}^{\mathrm{T}} \otimes \mathbf{I}_m\Big)\big(\boldsymbol{d}_r + \boldsymbol{a}_r\big)\Big], \end{aligned} \tag{36}$$

reducing the parametrization of Eq. (21) to

$$\begin{bmatrix} \boldsymbol{i}_{r;V^{\perp}} \\ \boldsymbol{\rho}_{r;V^{\perp}} \\ \boldsymbol{a}_{r;V^{\perp}} \\ \boldsymbol{d}_{r;V^{\perp}} \end{bmatrix} = \begin{bmatrix} \boldsymbol{i}_r \\ \boldsymbol{\rho}_r \\ \boldsymbol{a}_r \\ \boldsymbol{d}_r \end{bmatrix} - \mathbf{V}\begin{bmatrix} \boldsymbol{\beta}_1 \\ \boldsymbol{\beta}_2 \end{bmatrix} \ . \tag{37}$$

Considering the equality $\boldsymbol{x}_{r;V^{\perp}} = \mathbf{V}^{\perp}\boldsymbol{w}$, the estimable ambiguity and code-bias parameters $\boldsymbol{a}_{r;V^{\perp}}$ and $\boldsymbol{d}_{r;V^{\perp}}$ play the role of the *w* parameters, that is

$$\boldsymbol{w} \rightarrow \begin{bmatrix} \boldsymbol{a}_{r;V^{\perp}}^{\mathrm{T}}, \boldsymbol{d}_{r;V^{\perp}}^{\mathrm{T}} \end{bmatrix}^{\mathrm{T}} . \tag{38}$$

Similar to those of Eqs (25) and (31), the dimension of the above vector is $2fm$. The corresponding full-rank model follows by substituting Eq. (37) into Eq. (17). The model reads

$$E\left(\begin{bmatrix}\boldsymbol{\varphi}_r\\ \boldsymbol{p}_r\end{bmatrix}\right)=\left(\begin{bmatrix}\mathbf{I}+\boldsymbol{e}\boldsymbol{e}^{\mathrm{T}}+\boldsymbol{\mu}\boldsymbol{\mu}^{\mathrm{T}}, \boldsymbol{e}\boldsymbol{e}^{\mathrm{T}}-\boldsymbol{\mu}\boldsymbol{\mu}^{\mathrm{T}}\\ \boldsymbol{e}\boldsymbol{e}^{\mathrm{T}}-\boldsymbol{\mu}\boldsymbol{\mu}^{\mathrm{T}}, \mathbf{I}+\boldsymbol{e}\boldsymbol{e}^{\mathrm{T}}+\boldsymbol{\mu}\boldsymbol{\mu}^{\mathrm{T}}\end{bmatrix}\otimes\mathbf{I}_m\right)\begin{bmatrix}\boldsymbol{a}_{r;V^{\perp}}\\ \boldsymbol{d}_{r;V^{\perp}}\end{bmatrix}. \tag{39}$$

Compare this full-rank model with Eqs (26) and (32). As shown, only the estimable ambiguity and code bias parameters $\boldsymbol{a}_{r;V^{\perp}}$ and $\boldsymbol{d}_{r;V^{\perp}}$ are present in the model. Once they are computed, the solutions of $\boldsymbol{i}_{r;V^{\perp}}$, $\boldsymbol{\rho}_{r;V^{\perp}}$ follow from the equality $\boldsymbol{x}_{;V^{\perp}}=\mathbf{V}^{\perp}w$. Given the *w* parameters (Eq. (38)), the first row of $\boldsymbol{x}_{;V^{\perp}}=\mathbf{V}^{\perp}w$ gives (cf. Eq. (35))

$$\begin{aligned}\boldsymbol{i}_{r;V^{\perp}}&=\left(\boldsymbol{\mu}^{\mathrm{T}}\otimes\mathbf{I}_m\right)\left(\boldsymbol{d}_{r;V^{\perp}}-\boldsymbol{a}_{r;V^{\perp}}\right)\\ &=\frac{2\boldsymbol{\mu}^{\mathrm{T}}\boldsymbol{\mu}}{1+2\boldsymbol{\mu}^{\mathrm{T}}\boldsymbol{\mu}}\boldsymbol{i}_r+\frac{1}{1+2\boldsymbol{\mu}^{\mathrm{T}}\boldsymbol{\mu}}\left(\boldsymbol{\mu}^{\mathrm{T}}\otimes\mathbf{I}_m\right)\left(\boldsymbol{d}_r-\boldsymbol{a}_r\right).\end{aligned} \tag{40}$$

Compare the second expression with Eqs (28) and (34). In contrast to $\boldsymbol{i}_{r;S_1}$ and $\boldsymbol{i}_{r;S_2}$, the estimable parameter $\boldsymbol{i}_{r;V^{\perp}}$ does not follow as a straightforward 'biased' version of the unbiased ionospheric delays $\boldsymbol{i}_r$. Instead, its estimability reads a 'weighted-average' of $\boldsymbol{i}_r$ and $\left(\boldsymbol{\mu}^{\mathrm{T}}\otimes\mathbf{I}_m\right)\left(\boldsymbol{d}_r-\boldsymbol{a}_r\right)$. The weights are, respectively, given by $\left(2\boldsymbol{\mu}^{\mathrm{T}}\boldsymbol{\mu}\right)\Big/\left(1+2\boldsymbol{\mu}^{\mathrm{T}}\boldsymbol{\mu}\right)$ and $1\Big/\left(1+2\boldsymbol{\mu}^{\mathrm{T}}\boldsymbol{\mu}\right)$, adding up to unity.

4. GNSS DATA RELEVANT TO TEC SOLUTIONS

4.1. Estimable ionospheric delays of different precision

The above has shown that one can take an arbitrary $\mathcal{S}$-system (satisfying Eq. (7)) to form a full-rank version of the single-antenna model (17). Choosing three different $\mathcal{S}$-systems, we presented three different formulations of Eq. (17) having the following three different estimable ionospheric delays

$$\boldsymbol{i}_{r;S_1}\neq\boldsymbol{i}_{r;S_2}\neq\boldsymbol{i}_{r;V^{\perp}}. \tag{41}$$

For a quick reference, their estimablity and their solutions on the basis of one single observational epoch are given in Table 1. While the single-epoch code-leveled ionospheric solution $\hat{\boldsymbol{i}}_{r;S_1}$ is obtained by the GF combinations of the code-only data, the phase-leveled solution $\hat{\boldsymbol{i}}_{r;S_2}$ is a function of the phase-only data. As shown in the Table 1, the single-epoch solution $\hat{\boldsymbol{i}}_{r;V^{\perp}}$ is a function of the 'code-minus-phase' data. In terms of precision, they can be shown to be ordered as follows

Table 1. Estimability, single-epoch solution and interpretation of the estimable ionospheric delays formed by three different $\mathcal{S}$-systems.

	$\mathcal{S}$-System		
	Code-Leveled ($\mathbf{S}_1$)	Phase-Leveled ($\mathbf{S}_2$)	Minimum-Trace Variance Matrix ($\mathbf{V}^{\perp}$)
Estimability	$\boldsymbol{i}_{r;S_1} = \boldsymbol{i}_r + \boldsymbol{\mu}_{GF}^{\mathrm{T}} \boldsymbol{d}_r$	$\boldsymbol{i}_{r;S_2} = \boldsymbol{i}_r - \boldsymbol{\mu}_{GF}^{\mathrm{T}} \boldsymbol{a}_r$	$\boldsymbol{i}_{r;V^{\perp}} = \frac{2\boldsymbol{\mu}^{\mathrm{T}}\boldsymbol{\mu}}{1+2\boldsymbol{\mu}^{\mathrm{T}}\boldsymbol{\mu}} \boldsymbol{i}_r + \frac{1}{1+2\boldsymbol{\mu}^{\mathrm{T}}\boldsymbol{\mu}} \left(\boldsymbol{\mu}^{\mathrm{T}} \otimes \mathbf{I}_m\right)\left(\boldsymbol{d}_r - \boldsymbol{a}_r\right)$
Single-Epoch Solution	$\hat{\boldsymbol{i}}_{r;S_1} = +\boldsymbol{\mu}_{GF}^{\mathrm{T}} \boldsymbol{p}_r$	$\hat{\boldsymbol{i}}_{r;S_1} = -\boldsymbol{\mu}_{GF}^{\mathrm{T}} \boldsymbol{\varphi}_r$	$\hat{\boldsymbol{i}}_{r;V^{\perp}} = \frac{1}{1+2\boldsymbol{\mu}^{\mathrm{T}}\boldsymbol{\mu}} \left(\boldsymbol{\mu}^{\mathrm{T}} \otimes \mathbf{I}_m\right)\left(\boldsymbol{p}_r - \boldsymbol{\varphi}_r\right)$
Interpretation	Biased by DCBs	Biased by ambiguities	Weighted-average of $\boldsymbol{i}_r$ and code-biases/ambiguities

$$\mathbf{Q}_{\hat{i}_{r;S_2}\hat{i}_{r;S_2}} \leq \mathbf{Q}_{\hat{i}_{r;V^{\perp}}\hat{i}_{r;V^{\perp}}} \leq \mathbf{Q}_{\hat{i}_{r;S_1}\hat{i}_{r;S_1}} . \tag{42}$$

Now the question that comes to the fore is whether such precision dependency on the choice of $\mathcal{S}$-system can affect the final unbiased TEC solution $\hat{\boldsymbol{i}}_r$. In other words, should one prefer the phase-leveled solution $\hat{\boldsymbol{i}}_{r;S_2}$ to $\hat{\boldsymbol{i}}_{r;S_1}$ or $\hat{\boldsymbol{i}}_{r;V^{\perp}}$ as the input of TEC determination? If so, the differences between their corresponding TEC results must then be attributed to the usage of a nonrigorous estimation procedure. Our reasoning is as follows. All the three full-rank models (26), (32) and (39) follow by applying the one-to-one re-parametrization (20) to (17). Thus all the three models contain the same information. After all, it can be verified that the three stated solutions are linked by

$$\hat{\boldsymbol{i}}_{r;S_1} = \hat{\boldsymbol{i}}_{r;S_2} + \boldsymbol{\mu}_{GF}^{\mathrm{T}} \hat{\boldsymbol{d}}_{r;S_2} = \hat{\boldsymbol{i}}_{r;V^{\perp}} + \boldsymbol{\mu}_{GF}^{\mathrm{T}} \hat{\boldsymbol{d}}_{r;V^{\perp}} . \tag{43}$$

Working with any form of the estimable ionospheric parameters must therefore result in the same TEC outcome, provided that a properly weighted least-squares adjustment is employed. The quality of the TEC solution $\hat{\boldsymbol{i}}_r$ should not be judged on the basis of the precision of the ionospheric inputs $\hat{\boldsymbol{i}}_{r;S_1}$, $\hat{\boldsymbol{i}}_{r;S_2}$ or $\hat{\boldsymbol{i}}_{r;V^{\perp}}$ see e.g. (*Abdel-salam and Gao, 2004*; *Banville and Langley, 2011*). The following lemma presents a general rule on how the GNSS data propagate into an unbiased TEC solution.

Lemma 2 (Data of relevance for estimable functions): Let the design matrix $\mathbf{A}$ in Eq. (1) be partitioned as $\mathbf{A} = [\mathbf{A}_1, \mathbf{A}_2]$ with $\boldsymbol{x} = [\boldsymbol{x}_1^{\mathrm{T}}, \boldsymbol{x}_2^{\mathrm{T}}]^{\mathrm{T}}$, that is

$$E(\boldsymbol{y}) = \mathbf{A}_1\boldsymbol{x}_1 + \mathbf{A}_2\boldsymbol{x}_2 \ . \tag{44}$$

Would there exist an estimable parameter $\boldsymbol{u} = \mathbf{F}^{\mathrm{T}}\boldsymbol{x}_1$, then any linear unbiased estimator of $\boldsymbol{u}$ is a 'sole' function of $\mathbf{A}_2^{\perp\mathrm{T}}\boldsymbol{y}$, with $\mathbf{A}_2^{\perp}$ being a basis matrix of the orthogonal complement to $\mathbf{A}_2$. Proof is presented in the Appendix.

According to this lemma, one can eliminate the extra parameters $\boldsymbol{x}_2$ from the model by forming the linear combinations defined by $\mathbf{A}_2^{\perp\mathrm{T}}\boldsymbol{y}$. Pre-multiplying the model (44) $\mathbf{A}_2^{\perp\mathrm{T}}$, together with $\mathbf{A}_2^{\perp\mathrm{T}}\mathbf{A}_2 = 0$, gives

$$E\left(\mathbf{A}_2^{\perp\mathrm{T}}\boldsymbol{y}\right) = \left(\mathbf{A}_2^{\perp\mathrm{T}}\mathbf{A}_1\right)\boldsymbol{x}_1 \ . \tag{45}$$

We now apply Eq. (45) to the single-antenna model (17). As the estimable ionospheric delays are biased by combinations of $\boldsymbol{a}_r$ and $\boldsymbol{d}_r$ (cf. Table 1), we set the extra parameters as $\boldsymbol{x}_2 = [\boldsymbol{a}_r^{\mathrm{T}}, \boldsymbol{d}_r^{\mathrm{T}}]^{\mathrm{T}}$. The design matrix $\mathbf{A}_2$, along with $\mathbf{A}_2^{\perp}$, reads then

$$\mathbf{A}_2 = \begin{bmatrix} \mathbf{I}_{fm} & 0 \\ 0 & \mathbf{I}_{fm} \end{bmatrix} \Rightarrow \mathbf{A}_2^{\perp} = \{\ \} \text{ (an empty set).} \tag{46}$$

The above outcome clearly shows that the combined data $\mathbf{A}_2^{\perp\mathrm{T}}\boldsymbol{y} = \{\ \}$ contain no information about $\boldsymbol{x}_1 = [\boldsymbol{i}_r^{\mathrm{T}}, \rho_r^{\mathrm{T}}]^{\mathrm{T}}$. This makes sense, since both the GNSS data $\boldsymbol{\varphi}_r$ and $\boldsymbol{p}_r$ are reserved for the unknown parameters $\boldsymbol{a}_r$ and $\boldsymbol{d}_r$. As along as no extra information is available, one is therefore not able to provide an unbiased solution for the TEC parameters $\boldsymbol{i}_r$. Such GNSS-based extra information may be provided by accumulating data of multiple epochs which will be discussed in the following.

4.2. Time-differenced GNSS data

The single-epoch GNSS data were shown to contain no information on the unbiased TEC $\boldsymbol{i}_r$ due to the presence of the phase ambiguities $\boldsymbol{a}_r$ and the code biases $\boldsymbol{d}_r$ affecting the ionospheric estimability. The data of further epochs would therefore be of no use if the 'temporal' behaviour of $\boldsymbol{a}_r$ and $\boldsymbol{d}_r$ is unmodeled. The ambiguities $\boldsymbol{a}_r$ behave constant within the duration of a continuous satellite phase arc. Although the intra-day and daily changes of the code biases $\boldsymbol{d}_r$ have been reported (e.g., *Zhang and Teunissen, 2015*; *Jin et al., 2016*), they can be assumed stable during 1–3 days under the nominal conditions (*Sardon and Zarraoa, 1997*; *Schaer, 1999*; *Ciraolo et al., 2007*). From now on, we therefore assume $\boldsymbol{a}_r$ and $\boldsymbol{d}_r$ to be constant over k epochs, where k varies depending on the

applications and environmental conditions. The epoch argument t ($t = 1, \ldots, k$) is used to show the dependency of the other quantities on the observational epoch. The multi-epoch (k-epoch) version of the single-antenna model (17) then reads

$$E\left(\begin{bmatrix}\boldsymbol{\varphi}_r(t)\\ \boldsymbol{p}_r(t)\end{bmatrix}\right)=\left(\begin{bmatrix}-\boldsymbol{\mu},\boldsymbol{e}\\ +\boldsymbol{\mu},\boldsymbol{e}\end{bmatrix}\otimes\mathbf{I}_m\right)\begin{bmatrix}\boldsymbol{i}_r(t)\\ \boldsymbol{\rho}_r(t)\end{bmatrix}+\begin{bmatrix}\boldsymbol{a}_r\\ \boldsymbol{d}_r\end{bmatrix},$$
$$D\left(\begin{bmatrix}\boldsymbol{\varphi}_r(t)\\ \boldsymbol{p}_r(t)\end{bmatrix}\right)=\sigma_p^2\begin{bmatrix}\varepsilon\mathbf{I} & 0\\ 0 & \mathbf{I}\end{bmatrix}\otimes\mathbf{C}_t \tag{47}$$

for $t = 1, \ldots, k$. Similar to the single-epoch null-space identification presented in Section 3, one can identify the estimable ionospheric delays for multi-epoch versions of the previous three $\mathcal{S}$-systems.

Lemma 3 (Multi-epoch ionospheric estimability): Let $\boldsymbol{i}_r(\bar{t})$ be the arithmetic average of $\boldsymbol{i}_r(t)$ ($t = 1, \ldots, k$). Then the interpretation of estimable ionospheric delays $\boldsymbol{i}_{r;S_1}$ (in Eq. (28)), $\boldsymbol{i}_{r;S_2}$ (in Eq. (34)) and $\boldsymbol{i}_{r;V^\perp}$ (in Eq. (40)) are, respectively, extended to the multi-epoch case by

code-leveled (S_1)

$$\boldsymbol{i}_{r;S_1}(t)=\boldsymbol{i}_r(t)+\boldsymbol{\mu}_{GF}^{\mathrm{T}}\boldsymbol{d}_r\ , \tag{48}$$

phase-leveled (S_2):

$$\boldsymbol{i}_{r;S_2}(t)=\boldsymbol{i}_r(t)-\boldsymbol{\mu}_{GF}^{\mathrm{T}}\boldsymbol{a}_r\ , \tag{49}$$

minimum-trace variance matrix ($\mathbf{V}^\perp$):

$$\boldsymbol{i}_{r;V^\perp}(t)=\boldsymbol{i}_r(t)-\boldsymbol{i}_r(\bar{t})+\boldsymbol{i}_{r;V^\perp}(\bar{t})\ , \tag{50}$$

with

$$\boldsymbol{i}_{r;V^\perp}(\bar{t})=\frac{2\boldsymbol{\mu}^{\mathrm{T}}\boldsymbol{\mu}}{k+2\boldsymbol{\mu}^{\mathrm{T}}\boldsymbol{\mu}}\boldsymbol{i}_r(\bar{t})+\frac{1}{k+2\boldsymbol{\mu}^{\mathrm{T}}\boldsymbol{\mu}}\left[\left(\boldsymbol{\mu}^{\mathrm{T}}\otimes\mathbf{I}_m\right)\left(\boldsymbol{d}_r-\boldsymbol{a}_r\right)\right]\ . \tag{51}$$

Proof is presented in the Appendix.

Thus, despite the difference in the estimability of the three ionospheric parameters $\boldsymbol{i}_{r;S_1}$, $\boldsymbol{i}_{r;S_2}$ and $\boldsymbol{i}_{r;V^\perp}$, their 'time-differences' are identical, that is

$$\boldsymbol{i}_{r;S_1}(t)-\boldsymbol{i}_{r;S_1}(1)=\boldsymbol{i}_{r;S_2}(t)-\boldsymbol{i}_{r;S_2}(1)=\boldsymbol{i}_{r;V^\perp}(t)-\boldsymbol{i}_{r;V^\perp}(1)=\boldsymbol{i}_r(t)-\boldsymbol{i}_r(1)\ . \tag{52}$$

Their time-differences are equal to that of the unbiased TEC $\boldsymbol{i}_r(t)$.

The time-differences of all estimable ionospheric delays remain invariant for the choice of $\mathcal{S}$-system. This can be understood by an application of Lemma 2 to Eq. (47). We again set the extra parameters as $\boldsymbol{x}_2 = \left[\boldsymbol{a}_r^{\mathrm{T}}, \boldsymbol{d}_r^{\mathrm{T}}\right]^{\mathrm{T}}$, but now with the multi-epoch design matrix $\mathbf{A}_2$, and $\mathbf{A}_2^{\perp}$ as follows (compare with Eq. (46))

$$\mathbf{A}_2 = \boldsymbol{e}_k \otimes \begin{bmatrix} \mathbf{I}_{fm} & 0 \\ 0 & \mathbf{I}_{fm} \end{bmatrix} \Rightarrow \mathbf{A}_2^{\perp} = \mathbf{D}_k \otimes \begin{bmatrix} \mathbf{I}_{fm} & 0 \\ 0 & \mathbf{I}_{fm} \end{bmatrix}, \tag{53}$$

where the $k \times (k-1)$ matrix $\mathbf{D}_k$ is the between-epoch differencing operator, i.e. $\mathbf{D}_k^{\mathrm{T}} \boldsymbol{e}_k = 0$. For instance, when three epochs are considered ($k = 3$), $\mathbf{D}_3$ nullifies the summation vector $\boldsymbol{e}_k = [1, 1, 1]^{\mathrm{T}}$ as follows

$$\mathbf{D}_3^{\mathrm{T}} \boldsymbol{e}_3 = \begin{bmatrix} -1 & 1 & 0 \\ -1 & 0 & 1 \end{bmatrix} \begin{bmatrix} 1 \\ 1 \\ 1 \end{bmatrix} = \begin{bmatrix} 0 \\ 0 \end{bmatrix}. \tag{54}$$

Thus the combinations $\mathbf{A}_2^{\perp \mathrm{T}} \boldsymbol{y}$ are nothing else, but the time-differences of the phase and code data $\boldsymbol{\varphi}_r$ and $\boldsymbol{p}_r$, respectively. According to Lemma 2, any linear unbiased TEC solution is a function of these combinations only. The corresponding observation equations follow by time-differencing the first expression of Eq. (47) as

$$E\left(\begin{bmatrix} \boldsymbol{\varphi}_r(1t) \\ \boldsymbol{p}_r(1t) \end{bmatrix}\right) = \left(\begin{bmatrix} -\boldsymbol{\mu}, \boldsymbol{e} \\ +\boldsymbol{\mu}, \boldsymbol{e} \end{bmatrix} \otimes \mathbf{I}_m\right) \begin{bmatrix} \boldsymbol{i}_r(1t) \\ \boldsymbol{\rho}_r(1t) \end{bmatrix}, \tag{55}$$

with the shorthand notation $(\cdot)(1t) = (\cdot)(t) - (\cdot)(1)$, $t = 2, \ldots, k$. Since the above system of equations is full rank, one can evaluate the precision of the ionospheric solutions $\hat{\boldsymbol{i}}_r(1t)$.

Lemma 4 (Time-differenced ionospheric precision): In regard to the linear model (47), the (co)variance matrices of the least-squares solutions $\hat{\boldsymbol{i}}_r(1t)$ ($t = 2, \ldots, k$) are obtained as

$$C\left(\hat{\boldsymbol{i}}_r(1t), \hat{\boldsymbol{i}}_r(1l)\right) = \frac{\varepsilon \sigma_p^2}{f\gamma}(1+\varepsilon)\left(\mathbf{C}_1 + \delta_{tl}\mathbf{C}_t\right), \tag{56}$$

with

$$\gamma = (1+\varepsilon)^2 \sigma_{\mu}^2 + 4\varepsilon\bar{\mu}^2,$$

where

$$\bar{\mu} = \frac{1}{f}\sum_{j=1}^{f} \mu_j \quad \text{and} \quad \sigma_{\bar{\mu}}^2 = \frac{1}{f}\sum_{j=1}^{f} \left(\mu_j - \bar{\mu}\right)^2 .$$

The delta Kronecker is defined as $\delta_{tl} = 1$ for $t = l$ and $\delta_{tl} = 0$ for $t \neq l$. Proof is presented in the Appendix.

As shown in Eq. (56), the variance of the time-differenced solutions $\hat{\boldsymbol{i}}_r\left(1t\right)$ are governed by the phase variance $\sigma_\varphi^2 = \varepsilon\sigma_p^2$. Thus irrespective of the choice of $\mathcal{S}$-system, the time differenced solutions of all the estimable ionospheric delays of Eq. (47), including $\boldsymbol{i}_{r;S_1}$, $\boldsymbol{i}_{r;S_2}$ and $\boldsymbol{i}_{r;V^\perp}$, are of the phase-level precision.

5. ARRAY CONTRIBUTION TO TEC SOLUTIONS

Despite the phase-level precision of the time-differenced solutions $\hat{\boldsymbol{i}}_r\left(1t\right)$, it is well-known that GNSS TEC determination requires rather long observational time-span to achieve a standard-deviation less than 1 TECU (*Schaer, 1999*). Each TECU roughly corresponds to 16.2 cm experienced on GPS L1 signals. This seems to be at odds with the outcome of Lemma 4, since the precision of the input $\hat{\boldsymbol{i}}_r\left(1t\right)$ is at the millimeter-level. Such discrepancy is addressed by 1) the underlying ionospheric model linking the time-differenced ionospheric delays to their absolute versions, and 2) the geometry of the GNSS satellites that is known to change rather slowly over time.

Consider, for instance, the popular single layer model, see, e.g., *Schaer et al. (1995)*, *Mannucci et al. (1998)*, *Schaer (1999)*, *Komjathy et al. (2005)*, *Azpilicueta et al. (2006)*, *Brunini and Azpilicueta (2009, 2010)*. Accordingly the unbiased slant TEC is assumed to be mapped onto the so-called vertical TEC experienced on the radial direction of the ionospheric thin shell. The vertical TEC is further parameterized into unknown parameters, say $\boldsymbol{c}$, through a set of known basis functions. These time-dependent basis functions change as the satellite geometry with respect to the GNSS antenna changes. Let matrix $\mathbf{B}_t$ contain such time-dependent coefficients at epoch t. Given the ionospheric model $\boldsymbol{i}_r\left(t\right) = \mathbf{B}_t\boldsymbol{c}$, the unknown parameters $\boldsymbol{c}$ are determined through

$$E\left(\hat{\boldsymbol{i}}_r\left(1t\right)\right) = \left(\mathbf{B}_t - \mathbf{B}_1\right)\boldsymbol{c} \ . \tag{57}$$

Would the coefficient $\left(\mathbf{B}_t - \mathbf{B}_1\right)$ be small, the parameters $\boldsymbol{c}$ become poorly estimable. For example, in case of two consecutive epochs (with 30-s interval) of the 'biquadratic basis functions' (*Brunini and Azpilicueta, 2009*), we have

$$\left(\mathbf{B}_t - \mathbf{B}_1\right) \sim 10^{-4} \Rightarrow \sigma_{\hat{c}} \sim 10^4\,\sigma_\varphi \ , \tag{58}$$

where the sign '~' means 'is of the order of'. Thus the millimeter-level precision of the ionospheric input $\hat{\boldsymbol{i}}_r(1t)$ leads to TEC solutions with precision of about 60 TECU, showing the need of longer observational time spans.

In order to achieve high-precision TEC solutions within not too long observational time span, the idea is to incorporate the data of extra aiding antennas to GNSS TEC determination. Accordingly, $n-1$ additional antennas are setup in the vicinity of antenna r, forming an n-dimensional array of antennas. Such array-aided setup proves to be beneficial to GNSS precise positioning, carrier-phase ambiguity resolution, and integrity monitoring, see, e.g., *Teunissen (2012)*, *Li and Teunissen (2013)*, *Khodabandeh and Teunissen (2014, 2015b)*. The distances between the antennas are assumed to be short enough so that the same ionospheric delays, of each satellite, are experienced by all the antennas. Under such assumption, we have n independent sets of equations (55), each of which provides its own time-differenced solution $\hat{\boldsymbol{i}}_q(1t)$ ($q = 1, \ldots, n$), but with the conditions $\boldsymbol{i}_q(1t) = \boldsymbol{i}_r(1t)$ for all $q \neq r$. Thus the corresponding array-aided solution $\hat{\boldsymbol{i}}_r^{ARY}(1t)$ simply follows by averaging over the antennas, that is

$$\hat{\boldsymbol{i}}_r^{ARY}(1t) = \frac{1}{n}\sum_{q=1}^{n}\hat{\boldsymbol{i}}_q(1t) \ . \tag{59}$$

Combining the above result with Eqs (52) and (56), we therefore arrive at the following corollary.

Corollary (Array-aided ionospheric precision): Let S be an arbitrary $\mathcal{S}$-system of the model (47) with an n-dimensional array $r = 1, \ldots, n$. Assuming $\boldsymbol{i}_r(t) = \boldsymbol{i}_1(t)$ for all $r \neq 1$ ($t = 1, \ldots, k$), the (co)variance matrices of the least-squares solutions $\hat{\boldsymbol{i}}_{r;S}^{ARY}(1t)$ ($t = 2, \ldots, k$) are obtained as

$$C\left(\hat{\boldsymbol{i}}_r^{ARY}(1t), \hat{\boldsymbol{i}}_r^{ARY}(1l)\right) = \frac{\sigma_\varphi^2}{nf\gamma}(1+\varepsilon)\left(\mathbf{C}_1 + \delta_{tl}\mathbf{C}_t\right) \ , \tag{60}$$

with $\sigma_\varphi^2 = \varepsilon\sigma_p^2$ being the zenith-referenced variance of the phase data.

Thus while the results $\hat{\boldsymbol{i}}_{r;S}^{ARY}(1t)$ are invariant for the choice of $\mathcal{S}$-system, the variance of the corresponding TEC results retrieved gets n times smaller.

To get some numerical insight into the role played by the array-based setup in TEC determination, retrieved slant TEC's standard deviations of a GPS satellite (i.e. $\sigma_{\hat{i}_r}$) are presented in Table 2. The single-antenna results ($n = 1$) are compared with their array-aided counterparts ($n = 9$) for both the dual- and triple-frequency scenarios. These values represent the 'precision' of the solutions and not their 'accuracy'. Their accuracy can be further affected by the potential presence of the mis-modeled effects such as, e.g., multipath. As shown, the standard-deviations follow the $1/\sqrt{n}$ rule, that is, the array-

Table 2. Slant total electron content (TEC) standard deviations (in TECU) of a GPS satellite obtained by the 'biquadratic basis functions', with standard deviaition $\sigma_p \approx 1.85$ TECU and phase-to-code variance ratio $\varepsilon = 0.0001$. The results are presented for the number of epochs $k = 100$, 200 and 300 (sampling rate: 30 s, refreshing interval: 2.5 min). The single-antenna ($n = 1$) and array-aided ($n = 9$) modes are accompanied by the dual-frequency (L1/L2) and triple-frequency (L1/L2/L5) scenarios.

	Number of Epochs					
	100 (50 min)		200 (100 min)		300 (150 min)	
n	L1/L2	L1/L2/L5	L1/L2	L1/L2/L5	L1/L2	L1/L2/L5
1	1.461	1.119	1.210	0.927	0.905	0.693
9	0.487	0.373	0.403	0.309	0.302	0.231

aided standard deviations are 3 times smaller than their single-antenna versions. It is important to highlight that the TEC solutions, obtained by the array-aided triple-frequency within 50 minutes (0.373), are expected to be almost 2.4 times more precise than those of the single-antenna dual-frequency that are obtained within 150 minutes (0.905). This demonstrates that one can, using the array-based setup, speed up the observational time span required for obtaining high precision TEC results.

6. CONCLUSIONS

In this contribution we reviewed the $\mathcal{S}$-system theory and applied it to the rank-deficient GNSS observation equations. The null-space characterizing the lack of information content in the GNSS data was identified and the precision dependency of the estimable ionospheric parameters on the choice of $\mathcal{S}$-system was shown. With the choice of the $\mathcal{S}$-system being orthogonal complement to the null-space, the minimum-trace variance estimable parameters were also derived (cf. Fig. 2).

It was demonstrated why one should not fall into the trap of judging the precision of the retrieved TEC solutions on the basis of the precision of the estimable ionospheric input. Considering the time-constant ambiguities and code biases, we showed that only the time-differenced GNSS data are of relevance for TEC determination (cf. Eq. (53)). This was further corroborated by showing the invariance property of the time-differenced estimable ionospheric parameters for the choice of $\mathcal{S}$-system (cf. Eq. (52)).

Despite the phase-level precision of the time differenced ionospheric input (cf. Eq. (56)), TEC determination requires long observational time-span, as the geometry of the GNSS satellites changes rather slowly over time. We proposed the usage of an array of GNSS antennas, making the variance of the retrieved TEC outcomes n times smaller (cf. Eq. (60)), with n being the number of array antennas. This in turn expedites the long time-span required for high-precision TEC determination.

APPENDIX

Proof of Lemma 1. We first show that any **S** satisfying Eq. (7) can be expressed as

$$\mathbf{S} = \mathbf{V}^{\perp}\mathbf{X} + \mathbf{V}\left(\mathbf{YX}\right) \tag{A.1}$$

for some matrices **X** and **Y**, where **X** is invertible. Since $\mathbf{V}^{\perp}$ and **V** form a basis of the whole space $\mathbb{R}^n$ the columns of **S** are formed by linear combinations of $\mathbf{V}^{\perp}$ and **V**. Thus there exist some matrices **X** and **Z** such that

$$\mathbf{S} = \mathbf{V}^{\perp}\mathbf{X} + \mathbf{VZ} \ . \tag{A.2}$$

The square matrix **X** is invertible. If not, then there must be a non-zero vector $\boldsymbol{u}$ such that $\mathbf{X}\boldsymbol{u} = 0$. Pre-multiplying Eq. (A.2) by $\boldsymbol{u}$ gives $\mathbf{S}\boldsymbol{u} = \mathbf{VZ}\boldsymbol{u}$. But this implies $\mathbf{S}\boldsymbol{u} = 0$, since $\mathbf{S}\boldsymbol{u} \in \mathcal{R}\left(\mathbf{S}\right) \bigcap \mathcal{R}\left(\mathbf{V}\right) = \left\{0\right\}$. This is impossible as, by definition, **S** is a basis matrix (i.e. full-column rank). Thus **X** is invertible. Defining $\mathbf{Y} = \mathbf{ZX}^{-1}$, we get $\mathbf{Z} = \mathbf{YX}$, from which Eq. (A.1) follows. With $\mathbf{N} = \mathbf{A}^{\mathrm{T}}\mathbf{Q}_{yy}^{-1}\mathbf{A}$, substitution of Eq. (A.1) into Eq. (9) and taking the trace yields

$$\begin{aligned} \mathrm{tr}\left(\mathbf{Q}_{\hat{x}_{;S}\,\hat{x}_{;S}}\right) &= \mathrm{tr}\left(\mathbf{Q}_{\hat{x}_{;Y^{\perp}}\,\hat{x}_{;Y^{\perp}}}\right) + \mathrm{tr}\left(\left(\mathbf{VY}\right)\left(\mathbf{V}^{\perp\mathrm{T}}\mathbf{N}\mathbf{V}^{\perp}\right)^{-1}\left(\mathbf{VY}\right)^{\mathrm{T}}\right) \\ &\geq \mathrm{tr}\left(\mathbf{Q}_{\hat{x}_{;Y^{\perp}}\,\hat{x}_{;Y^{\perp}}}\right) \end{aligned} \tag{A.3}$$

since

$$\begin{aligned} \mathrm{tr}\left(\mathbf{V}^{\perp}\left(\mathbf{V}^{\perp\mathrm{T}}\mathbf{N}\mathbf{V}^{\perp}\right)^{-1}\left(\mathbf{VY}\right)^{\mathrm{T}}\right) &= \mathrm{tr}\left(\left(\mathbf{VY}\right)\left(\mathbf{V}^{\perp\mathrm{T}}\mathbf{N}\mathbf{V}^{\perp}\right)^{-1}\mathbf{V}^{\perp\mathrm{T}}\right) \\ &= \mathrm{tr}\left(\mathbf{V}^{\perp\mathrm{T}}\left(\mathbf{VY}\right)\left(\mathbf{V}^{\perp\mathrm{T}}\mathbf{N}\mathbf{V}^{\perp}\right)^{-1}\right) = 0 \, . \end{aligned} \tag{A.4}$$

As matrix $\left(\mathbf{V}^{\perp\mathrm{T}}\mathbf{N}\mathbf{V}^{\perp}\right)^{-1}$ is positive-definite, the second term of Eq. (A.3) vanishes if and only if $\mathbf{VY} = 0$, which is the case when $\mathbf{Y} = 0$, i.e. when $\mathcal{R}\left(\mathbf{S}\right) = \mathcal{R}\left(\mathbf{V}^{\perp}\right)$.

Proof of Lemma 2. Let $\mathbf{C}^{\mathrm{T}}\boldsymbol{y}$ be a linear unbiased estimator of $\boldsymbol{u} = \mathbf{F}^{\mathrm{T}}\boldsymbol{x}_1$. The unbiasedness condition, together with Eq. (44), gives

$$E\left(\mathbf{C}^{\mathrm{T}}\boldsymbol{y}\right) = \mathbf{C}^{\mathrm{T}}\mathbf{A}_1\boldsymbol{x}_1 + \mathbf{C}^{\mathrm{T}}\mathbf{A}_2\boldsymbol{x}_2 = \mathbf{F}^{\mathrm{T}}\boldsymbol{x}_1 \tag{A.5}$$

for all $\boldsymbol{x}_1$ and $\boldsymbol{x}_2$. This only holds when

$$\mathbf{A}_1^{\mathrm{T}}\mathbf{C} = \mathbf{F} \quad \text{and} \quad \mathbf{A}_2^{\mathrm{T}}\mathbf{C} = 0 \ , \tag{A.6}$$

where the second formula shows the necessary condition $\mathcal{R}\left(\mathbf{C}\right) \subset \mathcal{R}\left(\mathbf{A}_2^{\perp}\right)$.

Proof of Lemma 3. Let the parameter vector be ordered as $\boldsymbol{x} = \left[\boldsymbol{x}_{[k]}^{\mathrm{T}}, \boldsymbol{a}_r^{\mathrm{T}}, \boldsymbol{d}_r^{\mathrm{T}} \right]^{\mathrm{T}}$, where the vector $\boldsymbol{x}_{[k]}$ contains all the stacked vectors $\left[\boldsymbol{i}_r^{\mathrm{T}}(t), \boldsymbol{\rho}_r^{\mathrm{T}}(t) \right]^{\mathrm{T}}$ ($t = 1, \ldots, k$), respectively. The design matrix of Eq. (47) is then nullified by the basis matrix

$$\mathbf{V} = \begin{bmatrix} \boldsymbol{e}_k \otimes \mathbf{I}_{2m} \\ -\mathbf{A}_x \end{bmatrix}, \quad \text{with} \quad \mathbf{A}_x = \begin{bmatrix} -\boldsymbol{\mu}, \boldsymbol{e} \\ +\boldsymbol{\mu}, \boldsymbol{e} \end{bmatrix} \otimes \mathbf{I}_m \ . \tag{A.7}$$

The three $\mathcal{S}$-systems $\mathbf{S}_1$ (Eq. (22)), $\mathbf{S}_2$ (Eq. (29)) and $\mathbf{V}^{\perp}$ (Eq. (35)), respectively, take the following multi-epoch forms

$$\mathbf{S}_1 = \begin{bmatrix} \mathbf{I}_{2km} & 0 & 0 \\ 0 & \mathbf{I} \otimes \mathbf{I}_m & 0 \\ 0 & 0 & \mathbf{E} \otimes \mathbf{I}_m \end{bmatrix}, \tag{A.8}$$

$$\mathbf{S}_2 = \begin{bmatrix} \mathbf{I}_{2km} & 0 & 0 \\ 0 & \mathbf{E} \otimes \mathbf{I}_m & 0 \\ 0 & 0 & \mathbf{I} \otimes \mathbf{I}_m \end{bmatrix}, \tag{A.9}$$

$$\mathbf{V}^{\perp} = \begin{bmatrix} \mathbf{D}_k \otimes \mathbf{I}_{2m} & \dfrac{1}{f} \boldsymbol{e}_k \otimes \mathbf{A}_x^{\mathrm{T}} \\ 0 & \mathbf{I}_{2fm} \end{bmatrix}. \tag{A.10}$$

Substituting into the following $\mathcal{S}$-transformation (*Teunissen, 1985*)

$$\mathcal{S} = \mathbf{S}\left(\mathbf{V}^{\perp \mathrm{T}} \mathbf{S} \right)^{-1} \mathbf{V}^{\perp \mathrm{T}} \ , \quad \mathbf{S} = \begin{Bmatrix} \mathbf{S}_1 \\ \mathbf{S}_2 \\ \mathbf{V}^{\perp} \end{Bmatrix}, \tag{A.11}$$

the estimability of Eqs (48)–(50) follows then from the first rows of $\boldsymbol{x}_{;S} = \mathcal{S}\boldsymbol{x}$.

Proof of Lemma 4. We first eliminate $\boldsymbol{\rho}_r(1t)$ from the observation equations (55) through pre-multiplying them by the orthogonal-complement basis matrix

$$\left(\begin{bmatrix} \boldsymbol{e} \\ \boldsymbol{e} \end{bmatrix} \otimes \mathbf{I}_m \right)^{\perp \mathrm{T}} = \begin{bmatrix} -\mathbf{I} & +\mathbf{I} \\ \mathbf{D}_f^{\mathrm{T}} & \varepsilon \mathbf{D}_f^{\mathrm{T}} \end{bmatrix} \otimes \mathbf{I}_m \ , \tag{A.12}$$

giving the following two uncorrelated sets of equations

$$\begin{aligned} \boldsymbol{p}_r(1t) - \boldsymbol{\varphi}_r(1t) &= -2\left(\boldsymbol{\mu} \otimes \mathbf{I}_m \right) \boldsymbol{i}_r(1t), \\ \left(\mathbf{D}_f^{\mathrm{T}} \otimes \mathbf{I}_m \right) \left(\varepsilon \boldsymbol{p}_r(1t) + \boldsymbol{\varphi}_r(1t) \right) &= -(1-\varepsilon) \left(\mathbf{D}_f^{\mathrm{T}} \boldsymbol{\mu} \otimes \mathbf{I}_m \right) \boldsymbol{i}_r(1t). \end{aligned} \tag{A.13}$$

The normal matrices of the above two sets, respectively, read

$$\mathbf{N}_1 = \frac{4\boldsymbol{\mu}^{\mathrm{T}}\boldsymbol{\mu}}{(1+\varepsilon)\sigma_p^2}\left(\mathbf{C}_1 + \mathbf{C}_t\right)^{-1}, \quad \mathbf{N}_2 = \frac{(1-\varepsilon)^2\,\boldsymbol{\mu}^{\mathrm{T}}\mathbf{P}\boldsymbol{\mu}}{(1+\varepsilon)\sigma_\varphi^2}\left(\mathbf{C}_1 + \mathbf{C}_t\right)^{-1}, \tag{A.14}$$

where $\mathbf{P} = \mathbf{D}_f\left(\mathbf{D}_f^{\mathrm{T}}\mathbf{D}_f\right)^{-1}\mathbf{D}_f^{\mathrm{T}}$. The variance matrix of $\hat{\boldsymbol{i}}_r(1t)$ follows by inverting the sum of the normal matrices as

$$\left(\mathbf{N}_1 + \mathbf{N}_2\right)^{-1} = \frac{(1+\varepsilon)\sigma_\varphi^2}{f\gamma}\left(\mathbf{C}_1 + \mathbf{C}_2\right) \tag{A.15}$$

and the identities $\boldsymbol{\mu}^{\mathrm{T}}\boldsymbol{\mu} = f\left(\bar{\mu}^2 + \sigma_\mu^2\right)$ and $\boldsymbol{\mu}^{\mathrm{T}}\mathbf{P}\boldsymbol{\mu} = f\sigma_\mu^2$.

Acknowledgements: P.J.G. Teunissen is the recipient of an Australian Research Council (ARC) Federation Fellowship (Project Number FF0883188). This support is gratefully acknowledged.

References

Abdel-Salam M. and Gao Y., 2004. Precise GPS atmosphere sensing based on un-differenced observations. In: *Proceedings of the 17th International Technical Meeting of the Satellite Division of The Institute of Navigation (ION GNSS 2004)*. The Institute of Navigation, Manassas, VA, 933–940.

Azpilicueta F., Brunini C. and Radicella S., 2006. Global ionospheric maps from GPS observations using modip latitude. *Adv. Space Res.*, **38**, 2324–2331.

Baarda W., 1973. *S-Transformations and Criterion Matrices*. Technical Report. Publ. Geodesy, New Series, **5(1)**. Netherlands Geodetic Commission, Delft, The Netherlands (http://www.ncgeo.nl/phocadownload/18Baarda.pdf).

Banville S. and Langley R.B., 2011. Defining the basis of an integer-levelling procedure for estimating slant total electron content. In: *Proceedings of the 24th International Technical Meeting of the Satellite Division of The Institute of Navigation (ION GNSS 2011)*. The Institute of Navigation, Manassas, VA, Proceedings of ION GNSS 2011, Portland, OR, pp 2542–2551

Brunini C. and Azpilicueta F.J., 2009. Accuracy assessment of the GPS-based slant total electron content. *J. Geodesy*, **83**, 773–785.

Brunini C. and Azpilicueta F.J., 2010. GPS slant total electron content accuracy using the single layer model under different geomagnetic regions and ionospheric conditions. *J. Geodesy*, **84**, 293–304.

Ciraolo L., Azpilicueta F.J., Brunini C., Meza A. and Radicella S., 2007. Calibration errors on experimental slant total electron content (TEC) determined with GPS. *J. Geodesy*, **81**, 111–120.

Henderson H.V., Pukelsheim F. and Searle S.R., 1983. On the history of the Kronecker product. *Linear Multilinear Algebra*, **14**, 113–120.

Hernández-Pajares M., Zornoza J., Subirana J.S., Farnworth R. and Soley S., 2005. EGNOS test bed ionospheric corrections under the October and November 2003 storms. *IEEE Trans. Geosci. Remote Sensing*, **43**, 2283–2293.

Jin S.G., Jin R. and Li D., 2016. Assessment of BeiDou differential code bias variations from multi-GNSS network observations. *Ann. Geophys.*, **34**, 259–269.

Khodabandeh A. and Teunissen P.J.G., 2014. Array-based satellite phase bias sensing: theory and GPS/BeiDou/QZSS results. *Meas. Sci. Technol*., **25**, 095801.

Khodabandeh A. and Teunissen P.J.G., 2015a. An analytical study of PPP-RTK corrections: precision, correlation and user-impact. *J. Geodesy*, **89**, 1109–1132.

Khodabandeh A. and Teunissen P.J.G., 2015b. Single-epoch GNSS array integrity: an analytical study. In: Sneeuw N., Novák P., Crespi M. and Sansò F. (Eds), *VIII Hotine-Marussi Symposium on Mathematical Geodesy*. International Association of Geodesy Symposia, **142**. Springer International Publishing, Cham, Switzerland, 263–272.

Khodabandeh A. and Teunissen P.J.G., 2016. Array-aided multifrequency GNSS ionospheric sensing: estimability and precision analysis. *IEEE Trans. Geosci. Remote Sensing*, **54,** 5895–5913.

Komjathy A., Sparks L., Wilson B.D. and Mannucci A.J., 2005. Automated daily processing of more than 1000 ground based GPS receivers for studying intense ionospheric storms. *Radio Sci.*, **40**, RS6006.

Li B. and Teunissen P.J.G., 2013. GNSS antenna array-aided CORS ambiguity resolution. *J. Geodesy*, **88**, 363–376.

Mannucci A., Wilson B., Yuan D., Ho C., Lindqwister U. and Runge T., 1998. A global mapping technique for GPS-derived ionospheric total electron content measurements. *Radio Sci.*, **33**, 565–582.

Sardon E. and Zarraoa N., 1997. Estimation of total electron content using GPS data: How stable are the differential satellite and receiver instrumental biases? *Radio Sci.*, **32**, 1899–1910.

Sardon E., Rius A. and Zarraoa N., 1994. Estimation of the transmitter and receiver differential biases and the ionospheric total electron content from Global Positioning System observations. *Radio Sci.*, **29**, 577–586.

Schaer S., 1999. *Mapping and Predicting the Earth's Ionosphere Using the Global Positioning System*. PhD Thesis. University of Bern, Bern, Switzerland.

Schaer S., Beutler G., Mervart L., Rothacher M. and Wild U., 1995. Global and regional ionosphere models using the GPS double difference phase observable. In: Gendt G. and Dick G. (Eds), *IGS Workshop Proceedings: Special Topics and New Directions*. GeoForschungsZentrum, Potsdam, Germany, 77–92.

Teunissen P.J.G., 1985. Generalized inverses, adjustment, the datum problem and S-transformations. In: Grafarend E.W. and Sansò F. (Eds), *Optimization and Design of Geodetic Networks*. Springer-Verlag, Berlin, Heidelberg, Germany.

Teunissen P.J.G., 2012. A-PPP: array-aided precise point positioning with global navigation satellite systems. *IEEE Trans. Signal Process.*, **60**, 2870–2881.

Yue X., Schreiner W.S., Kuo Y.H., Braun J.J., Lin Y.C. and Wan W., 2014. Observing system simulation experiment study on imaging the ionosphere by assimilating observations from ground GNSS, LEO-based radio occultation and ocean reflection, and cross link. *IEEE Trans. Geosci. Remote Sensing*, **52**, 3759–3773.

Zhang B. and Teunissen P.J.G., 2015. Characterization of multi-GNSS between-receiver differential code biases using zero and short baselines. *Sci. Bull.*, **60**, 1840–1849.